

A COMPARISON OF ANGULAR DISCRETIZATION TECHNIQUES FOR THE RADIATIVE TRANSPORT EQUATION

John Tencer

Sandia National Laboratories
 Albuquerque, NM, USA

ABSTRACT

Two of the most popular deterministic radiation transport methods for treating the angular dependence of the radiative intensity for heat transfer: the discrete ordinates and simplified spherical harmonics approximations are compared. A problem with discontinuous boundary conditions is included to evaluate ray effects for discrete ordinates solutions. Mesh resolution studies are included to ensure adequate convergence and evaluate the effects of the contribution of false scattering. All solutions are generated using finite element spatial discretization. Where applicable, any stabilization used is included in the description of the approximation method or the statement of the governing equations. A previous paper by the author presented results for a set of 2D benchmark problems for the discrete ordinates method using the PN-TN quadrature of orders 4, 6, and 8 as well as the P1, M1, and SP3 approximations. This paper expands that work to include the Lathrop-Carlson level symmetric quadrature of order up to 20 as well as the Lebedev quadrature of order up to 76 and simplified spherical harmonics of odd orders from 1 to 15. Two 3D benchmark problems are considered here. The first is a canonical problem of a cube with a single hot wall. This case is used primarily to demonstrate the potentially unintuitive interaction between mesh resolution, quadrature order, and solution error. The second case is meant to be representative of a pool fire. The temperature and absorption coefficient distributions are defined analytically. In both cases, the relative error in the radiative flux or the radiative flux divergence within a volume is considered as the quantity of interest as these are the terms that enter into the energy equation. The spectral dependence of the optical properties and the intensity is neglected.

NOMENCLATURE

μ_n is the nth quadrature point in a (N+1)-point Gauss set

on [-1, 1]

I_n is the angular intensity at quadrature point n
 σ_T is the macroscopic total cross section or extinction coefficient

ϕ is the angle-integrated intensity $\phi = 4\pi \sum_{m=1}^{(N+1)/2} w_m I_m$

w_n is the nth quadrature weight

σ_s is the macroscopic scattering cross section or scattering coefficient

σ_a is the macroscopic absorption cross section or absorption coefficient

σ is the Stefan-Boltzmann constant

T is the material temperature

I_b is the black-body intensity $I_b = \frac{\sigma T^4}{\pi}$

$\vec{\Omega}_i$ is a unit vector pointing in the ordinate direction corresponding to quadrature point i

ε is the surface emissivity

\vec{n} is the surface normal unit vector

INTRODUCTION

Radiation transport is an important phenomenon occurring in many physical systems. In heat transfer applications, this typically consists of the transport of relatively low energy photons through a translucent material. Photons may be emitted, absorbed, and scattered within the medium and at the boundary surfaces. The material properties corresponding to these processes are the surface emissivity and the absorption and scattering cross-sections of the medium. The radiative transport equation (Equation 1) governs the exchange or thermal radiation through a participating medium.

$$\vec{\Omega} \cdot \vec{\nabla} I(\vec{\Omega}) + (\sigma_A + \sigma_S)I(\vec{\Omega}) = \sigma_A I_b + \frac{\sigma_S}{4\pi} \int I(\vec{\Omega}) d\vec{\Omega} \quad (1)$$

In its most general form, the radiative transport equation has seven independent variables in space (3), direction (2), energy (1), and time (1). Equation 1 is written in steady-state because the time scales involved in the propagation of thermal radiation is much smaller than the other time scales of interest in a typical coupled heat transfer problem. In heat transfer applications, quantities of interest such as the radiative heat flux and the divergence of the radiative flux involve integrations over direction and energy and consequently vary only spatially and temporally. Setting aside the considerable complexity of the spectral dependence, this paper focuses on the techniques commonly used to approximate the angular dependence of the intensity.

Several of the most popular deterministic radiation transport methods for heat transfer including discrete ordinates, spherical harmonics, and simplified spherical harmonics are compared. A previous paper by the author [1] presented results for a set of 2D benchmark problems for the discrete ordinates method using the PN-TN quadrature of orders 4, 6, and 8 as well as the P1, M1, and SP3 approximations. This paper expands that work to include the Lathrop-Carlson level symmetric quadrature of order up to 20 as well as the Lebedev quadrature of order up to 76 and simplified spherical harmonics of odd order from 1 to 15. Unlike the previous work, in this paper fully 3D benchmark problems which more accurately mimic practical use cases are considered and used to evaluate the accuracy of the various angular approximations. Special attention is paid to the unintuitive interaction between order and mesh resolution for discrete ordinates solutions in the presence of ray effects.

DISCRETE ORDINATES

The discrete ordinates method is the most popular deterministic method for approximating radiative transport in participating media. In the discrete ordinates method, the radiative intensity is evaluated in a finite number of “ordinate directions.” These directions are chosen so that they correspond to the integration points in a given quadrature rule over the unit sphere. This quadrature is then used to evaluate integral quantities such as the angle-integrated intensity and the radiative heat flux. The discrete ordinates method enjoys wide adoption because the derivation [2, 3, 4, 5, 6, 1] is intuitive and the solution is guaranteed to converge to the correct solution as the number of ordinate directions considered approaches infinity.

The discrete ordinates method reduces Equation 1 into a set of N first order linear differential equations (one for each of the N ordinate directions in the chosen quadrature rule).

$$\vec{\Omega}_i \cdot \vec{\nabla} I_i + (\sigma_A + \sigma_S) I_i = \sigma_A I_b + \frac{\sigma_S}{4\pi} \sum w_j I_j \quad (2)$$

The corresponding boundary conditions for gray-diffuse walls is

$$I_i = \varepsilon I_{bw} + \frac{1-\varepsilon}{\pi} \sum_{\vec{n} \cdot \vec{\Omega}_j < 0} w_j I_j |\vec{n} \cdot \vec{\Omega}_j| \quad (3)$$

The boundary condition (Equation 3) is only applied to the intensity leaving a given surface, i.e. if $\vec{n} \cdot \vec{\Omega}_j > 0$. The set of first-order discrete ordinates equations may be manipulated into various second-order forms if desired. A great deal of research over the last several decades has gone into finding stable and computationally efficient ways to solve the discrete ordinates equations.

SIMPLIFIED SPHERICAL HARMONICS

The simplified spherical harmonics or SPn angular approximation technique was first proposed by Gelbard in the early 1960s [7, 8, 9] as an ad hoc extension of the one-dimensional spherical harmonics approximation into three dimensions. The SPn equations have since been more rigorously derived from an asymptotic expansion of the P1 or diffusion approximation and from the use of particular trial functions in the self-adjoint variational characterization of the even-parity form of the radiative transfer equation [10, 11]. The SP1 approximation is equivalent to the P1 approximation.

Use of the SPn approximation within the nuclear engineering community has grown steadily over the past 20 years [12, 13, 14]. More recently, the method has begun growing in popularity for heat transfer applications [15, 16, 17]. Because the SPn equations may be derived in so many different ways, there are a large number of equivalent forms in common use. The “canonical” form [18, 1] derived from the 1D even-parity discrete ordinates equations is a set of coupled diffusion equations given by

$$\vec{\nabla} \cdot \left(\frac{\mu_i^2}{(\sigma_A + \sigma_S)} \vec{\nabla} I_i \right) + (\sigma_A + \sigma_S) I_i = \sigma_A I_b + \frac{\sigma_S}{4\pi} \phi \quad (4)$$

The preponderance of published results in the heat transfer community use the Marshak boundary condition for the SPn equations. The Marshak condition is considered more accurate for low order approximations but involves additional coupling of the SPn equations at the boundaries. However, in this work we employ the Mark boundary condition which has the advantage of not coupling the SPn diffusion equations at the boundary in the case of black walls. The Mark boundary condition approaches the Marshak boundary condition as the approximation order increases.

$$-\frac{\mu_i}{\sigma_A + \sigma_S} \vec{\nabla} I_i \cdot \vec{n} = \frac{\varepsilon}{2 - \varepsilon} (I_i - I_{bw}) + \frac{1-\varepsilon}{2-\varepsilon} \left[\frac{\sum (I_k - \frac{\mu_k}{\sigma_A + \sigma_S} \vec{\nabla} I_k \cdot \vec{n}) \mu_k w_k}{\sum \mu_k w_k} - I_i + \frac{\mu_i}{\sigma_A + \sigma_S} \vec{\nabla} I_i \cdot \vec{n} \right] \quad (5)$$

The discrete ordinates solutions presented in this paper are generated using the SCEPTRE suite of codes for solving the linear steady-state Boltzmann transport equation [19]. The simplified spherical harmonics solutions are computed using Sierra Aria, a thermal analysis code that is highly scalable [20].

CASE 1

In previous work the infinitely long square duct with a single wall was considered [1]. The analytical solution of Crosbie and Schrenker [21] was used as a benchmark. This technique was later expanded to inhomogeneous media with isotropic scattering by Altac and Tekkalmaz [22]. Here we consider the three-dimensional analog to this problem: A cube with one side ($z=1$) heated. Our quantities of interest are the angle-integrated intensity and the heat flux perpendicular to the heated wall as a function of the distance from the heated wall along the centerline. The geometry for Case 1 is illustrated in Figure 1.

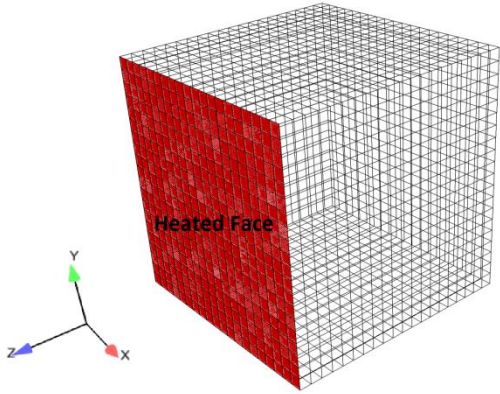


Figure 1: Geometry for Case 1. Cold Cube with black walls, one wall heated uniformly.

Uniform grids of $20 \times 20 \times 20$, $40 \times 40 \times 40$, and $80 \times 80 \times 80$ are used to assess mesh convergence. As a benchmark solution, a very high order discrete ordinates solution on the finest grid is used. Ray effect errors dominate all other sources of error for this scenario. Ray effects are errors resulting from the angular discretization used in the discrete ordinates method. They are propagations of discontinuities along the finite set of ordinate directions and manifest themselves as spurious oscillations in the quantities of interest. Scattering mitigates ray effects by smoothing out discontinuities as the rays traverse the domain. Gray (rather than black) walls also mitigate ray effects by added internal reflections. For this reason, a purely absorbing media (no scattering) with black walls is expected to produce the largest errors. For the results shown here, the optical side-length is set to unity. Relative errors are expected to be larger for larger optical thicknesses.

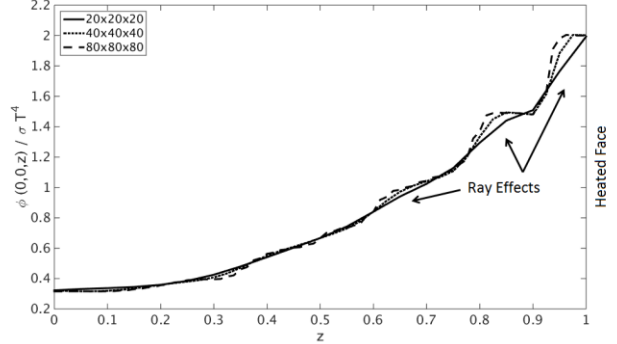


Figure 2: Angle-integrated intensity distribution along the centerline using the 18th order level-symmetric quadrature (360 ordinate directions) on several meshes.

Ray effects are still apparent in the S18 solution on the finest mesh (Figures 2 and 3). These oscillations are less apparent on the coarser meshes due to false scattering. False scattering is a numerical smearing of the solution due to insufficient mesh resolution. This is a characteristic common to problems of this type. Because false scattering effects compensate for ray effects, mesh refinement without a corresponding increase in angular resolution can actually decrease accuracy. Mesh resolution and angular resolution are not independent and must be varied together in order to increase solution accuracy.

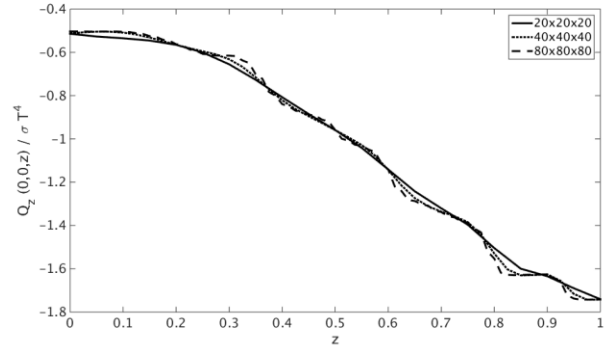


Figure 3: Heat flux away from hot wall along centerline using the 18th order level-symmetric quadrature (360 ordinate directions) on several meshes.

In the angle-integrated intensity distribution, the ray effects are most noticeable near the hot surface ($z=1$). This is true for quadratures with large numbers of ordinates but not necessarily for lower order quadratures. As seen in Figure 3, the oscillations in the heat flux are less pronounced and more evenly distributed throughout the volume. The level-symmetric quadrature only allows orders up to 20 (440 ordinate directions). In order to effectively eliminate ray effects from the solution on the fine mesh higher orders are required. The Lebedev quadrature allows for the inclusion of significantly more ordinate directions. The Lebedev quadrature of order 58 contains 1202 ordinate directions. On the finest meshes, this

still results in a solution with visibly noticeable ray effects. However, ray effects are not noticeable on the 40x40x40 mesh for this quadrature. As can be seen in Figures 4 and 5 the solution is significantly less dependent on mesh resolution for quadratures of this high of an order.

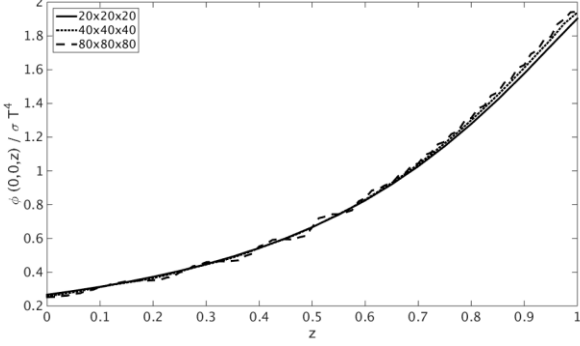


Figure 4: Angle-integrated intensity distribution along the centerline using the 58th order Lebedev quadrature on several meshes

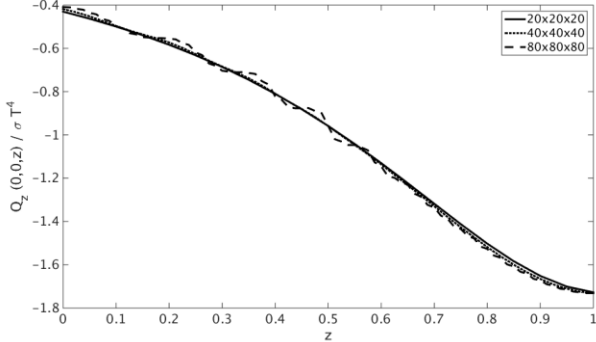


Figure 5: Heat flux away from hot wall along centerline the 58th order Lebedev quadrature on several meshes

Looking at the convergence with mesh refinement shows increased accuracy in solving the discrete ordinates equation set of a given order. However, since this equation set is an approximation of the real system and its solution is polluted by ray effects (angular discretization errors), increasing mesh resolution does not result in increased accuracy relative to the true solution. Instead, mesh refinement (beyond a certain point) only serves to better resolve the nonphysical oscillations known as ray effects.

The 76th order Lebedev quadrature contains 2030 ordinate directions and does not exhibit ray effects on the 80x80x80 mesh. It is therefore chosen to be sufficiently close to the true solution for this problem to be used to assess the error in the lower-order approximations. Looking at the L2 error in the quantities of interest (angle-integrated intensity and heat flux along the centerline) it is apparent that the number of ordinate directions used is the dominant term in the error. Figure 6 shows the L2 error in the angle-integrated intensity as a

function of the number of ordinate directions for the Lathrop-Carlson and Lebedev quadratures.

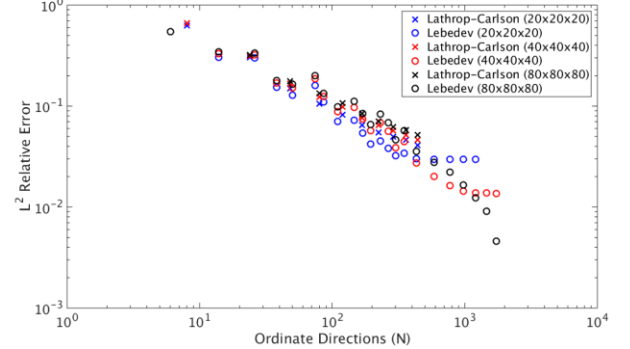


Figure 6: L2 error in the angle-integrated intensity relative to the 76th order Lebedev quadrature solution on the finest mesh as a function of mesh size and number of ordinate directions.

The error in the heat flux demonstrates similar behavior to that observed in the error in the angle-integrated intensity. For low numbers of ordinate directions, mesh refinement enhances the ray effects and actually reduces the accuracy of the solution. Only for very large numbers of ordinate directions does mesh refinement improve solution accuracy, and even there it is expected that eventually further refinement would have deleterious effect. As seen in Figures 2, 3 and 6, the level symmetric Lathrop-Carlson quadrature is insufficient to fully resolve the ray effects in this problem. However, it is noted that the Lathrop-Carlson quadrature often outperforms the Lebedev quadrature of comparable size for smaller numbers of ordinate directions. For more realistic problems with less pronounced ray effects or for applications where a very large quadrature set is impractical the Lathrop-Carlson quadrature appears to be a reasonable choice.

The relative error in the simplified spherical harmonics (SPn) approximation is summarized in Figure 7. The SPn approximation always yields a smooth solution but unlike the discrete ordinates method it is not guaranteed to converge to the correct answer as the order approaches infinity in multidimensional geometries. In fact, for this particular geometry where the solution is both highly directional and fully 3D, the error in the SPn solution increases with increasing order.

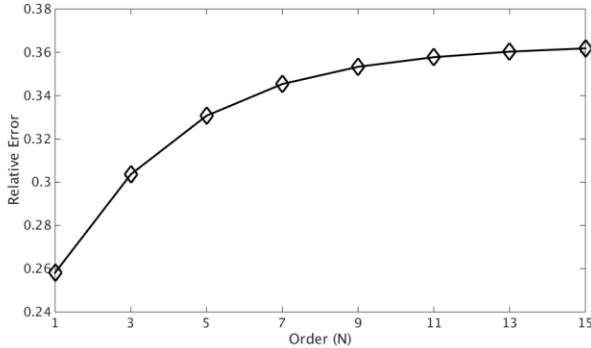


Figure 7: Relative L^2 error in the angle-integrated intensity distribution along the centerline using the SP n approximation as a function of approximation order.

In this case, the SP n approximation converges to a solution that is in excess of 30% error. At all orders, the SP n approximation under predicts the angle-integrated intensity along the centerline for this case. The SP n approximation is expected to perform better for applications that are more approximately 1D as well as problems with significant scattering where the intensity is expected to be closer to isotropic. The second test case attempts to test this hypothesis.

CASE 2

The second test case involves a cylindrical geometry with temperature and optical property distributions intended to be representative of those encountered in a pool fire. The problem is radially symmetric. The temperature distribution is given by

$$T(r, z) = 300 + 700 \begin{cases} [1 - (r - 0.8)^2] e^{-10(3(r-1)^2 - z)^2} & r < 0.8 \\ \left[1 - \left(\frac{r-0.8}{0.2}\right)^2\right] e^{-10(3(r-1)^2 - z)^2} & 0.8 \leq r < 1 \\ 0 & r \geq 1 \end{cases} \quad (6)$$

The absorption coefficient is defined as

$$\sigma_a = 10e^{-3r^2} \quad (7)$$

This temperature distribution is radially symmetric and is pictured in Figure 8.

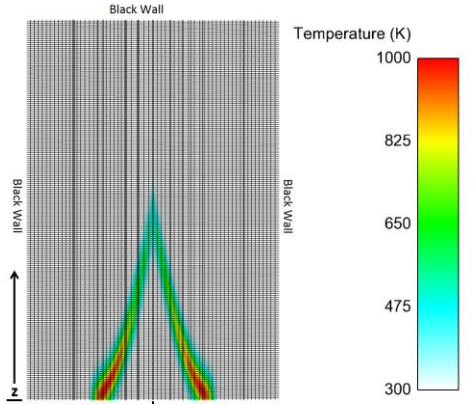


Figure 8: Temperature distribution for Case 2

The walls are black with temperature given by equation 6. The bounding surface is a cylinder of radius 2 and height 6. The quantity of interest for Case 2 is the angle-integrated intensity along the axis of this cylinder. This particular quantity is chosen because it does not demonstrate the radical ray effect behavior investigated by case 1. Figure 9 shows the value for the angle-integrated intensity as a function of z .

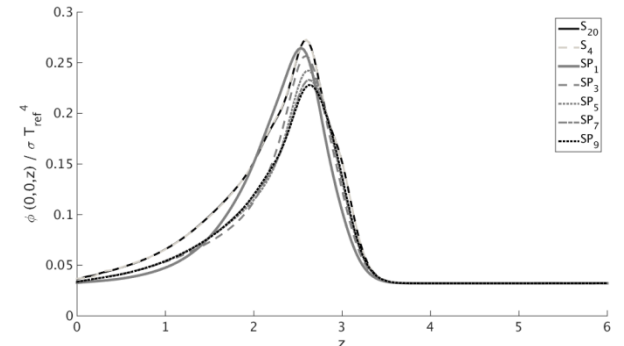


Figure 9: Angle-integrated intensity distribution for Case 2 using the simplified spherical harmonics approximation and discrete ordinates method of various orders.

Ray effects are drastically reduced in this case as can be seen by the lack of spurious oscillations in the S4 and S20 solutions plotted above. Consequently, the discrete ordinates method converges rapidly. The S4 (24 ordinate directions) is almost indistinguishable from the S20 (440 ordinate directions) solution. Note that this is true because the quantity of interest for this case is the angle-integrated intensity along the centerline. Ray effects remain noticeable in other solution regions away from the flame. In regions far from the flame, the solution behaves similarly to that in case 1. Figure 10 shows the convergence of the L^2 norm of our quantity of interest as the angular resolution is increased.

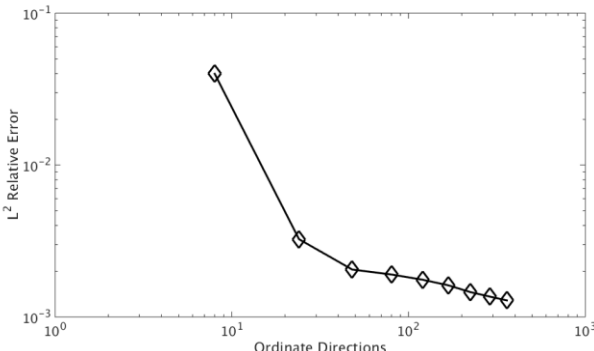


Figure 10: Relative L^2 error in the angle-integrated intensity distribution along the centerline using the discrete ordinates method with the Lathrop-Carlson level-symmetric quadrature as a function of the number of ordinate directions included

The discrete ordinates method performs very well for predicting the quantity of interest for this case. The Lebedev quadrature performs similarly for this case and is not pictured above. The extremely large quadratures used in Case 1 are seen to be of limited value for Case 2. Because of the lack of ray effects, this is not expected to change significantly with further mesh refinement.

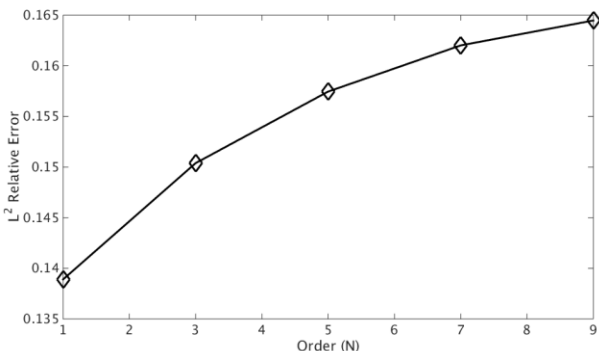


Figure 11: Relative L^2 error in the angle-integrated intensity distribution along the centerline using the SP n approximation as a function of approximation order.

Figure 11 shows the behavior of the L^2 norm of our quantity of interest for the simplified spherical harmonics approximation as the approximation order is increased. The simplified spherical harmonics approximation is seen to visually converge by order 9 but once again, increases in the approximation order result in decreases in solution accuracy. However, in this case the change in error is smaller and the overall error is about half of what it was case 1.

The simplified spherical harmonics approximation is thought to perform better in this case because although the solution is still not remotely 1D, the intensity is more isotropic than in Case 1 due to the volumetrically distributed source. The method would be expected to perform even better in the presence of scattering. The 15% relative error in the angle-integrated intensity is likely acceptable for many applications

when considered along with other simplifying assumptions such as neglecting spectral effects.

CONCLUSIONS

Ray effects dominate the discrete ordinates solution in the first case. These effects are partially mitigated by false scattering on coarser meshes. In order to observe a benefit from mesh refinement a very large quadrature set is required. Quadrature sets of this size are seldom used in practical heat transfer applications due to computational constraints. A general guideline appears to be that if ray effects are visually apparent in the solution further mesh refinement will likely reduce solution accuracy rather than improve it and should be avoided. The simplified spherical harmonics approximation yields an error of about 30% for the first case. This is a large error relative to what may be achieved with the discrete ordinates method. However, the simplified spherical harmonics approximation is much more computationally efficient and may be acceptable for a number of applications. No benefit is observed by increasing the order of the simplified spherical harmonics approximation for this case.

The second case is more realistic and is meant to resemble the distributions within an axially symmetric flame. The angle-integrated intensity along the centerline which corresponds to the radiative source term in the energy equation is chosen as the quantity of interest for Case 2. This quantity is not as susceptible to ray effects as other potential choices (radiative heat flux some distance away from the flame). The discrete ordinates method performs very well in calculating this quantity even for low numbers of ordinate directions. The simplified spherical harmonics approximation yields about a 15% error in this quantity of interest which is likely acceptable for many applications. Once again, no benefit is observed by increasing the order of the simplified spherical harmonics approximation. For the two cases considered, the error is minimized by choosing the lowest order approximation which is equivalent to the lowest order spherical harmonics approximation and assumes an isotropic radiative intensity.

A general guideline appears to be that mesh refinement is only worthwhile if the solution on the current mesh does not exhibit any visible ray effects (unphysical oscillations). If the solution is polluted by ray effects, computational resources are likely best used in mitigating these effects. In cases where further angular refinement is impractical mesh coarsening may even be appropriate. This paper did not consider the influence of optical thickness or scattering albedo in detail. Both of these parameters are known to influence the conclusions reached. No value was found in increases the SP n approximation order for either of the cases considered here. However, this is not thought to be true generally. Effective use of the SP n approximation for heat transfer problems remains an area of active research.

ACKNOWLEDGMENTS

Sandia National Laboratories is a multi-program laboratory managed and operated by Sandia Corporation, a wholly owned

subsidiary of Lockheed Martin Corporation, for the U.S. Department of Energy's National Nuclear Security Administration under contract DE-AC04-94AL85000. This document has been reviewed and approved for unclassified, unlimited release under 2015-####

REFERENCES

- [1] J. Tencer and J. R. Howell, "A parametric study of the accuracy of several radiative transport solution methods for a set of 2-D benchmark problems," in *Proceedings of the ASME 2013 Summer Heat Transfer Conference*, Minneapolis, MN, USA, 2013.
- [2] E. E. Lewis and W. F. Miller, Jr., *Computational Methods of Neutron Transport*, La Grange Park, Illinois: American Nuclear Society, Inc., 1993.
- [3] M. F. Modest, *Radiative Heat Transfer*, New York, New York: McGraw-Hill, Inc., 1993.
- [4] R. Siegel and J. R. Howell, *Thermal Radiation Heat Transfer*, New York, New York: Taylor & Francis, 2002.
- [5] J. Y. Murthy and S. R. Mathur, "Finite volume method for radiative heat transfer using unstructured meshes," *Journal of Thermophysics and Heat Transfer*, vol. 12, no. 3, 1998.
- [6] S. H. Kang and T. H. Song, "Finite element formulations of the first- and second-order discrete ordinates equations for radiative heat transfer calculation in three-dimensional participating media," *Journal of Quantitative Spectroscopy and Radiative Transfer*, vol. 109, pp. 2094-2107, 2008.
- [7] E. M. Gelbard, "Westinghouse Report No. WAPD-BT-20," 1960.
- [8] E. M. Gelbard, "Westinghouse Report No. WAPD-T-1182," 1961.
- [9] E. M. Gelbard, "Westinghouse Report No. WAPD-TM-294," 1962.
- [10] E. W. Larsen, J. E. Morel and J. M. McGhee, "Asymptotic Derivation of the Simplified Pn Equations," in *Proceedings of Joint International Conference on Mathematical Methods and Supercomputing in Nuclear Applications*, Karlsruhe, Germany, 1993.
- [11] G. C. Pomraning, "Asymptotic and Variational Derivations of the Simplified Pn Equations," *Ann. Nucl. Energy*, vol. 20, no. 9, pp. 623-637, 1993.
- [12] J. A. Josef and J. E. Morel, "Simplified Spherical Harmonic Method for Coupled Electron-Photon Transport Calculations," *Physical Review E*, vol. 57, no. 5, pp. 6161-6171, 1998.
- [13] P. S. Brantley and E. W. Larsen, "The Simplified P3 Approximation," *Nuclear Science and Engineering*, vol. 134, pp. 1-21, 2000.
- [14] R. Ciolini, G. G. M. Coppa, B. Montagnini and P. Ravetto, "Simplified Pn and An Methods in Neutron Transport," *Progress in Nuclear Energy*, vol. 40, no. 2, pp. 237-264, 2002.
- [15] M. F. Modest and S. Lei, "The Simplified Spherical Harmonics Method for Radiative Heat Transfer," in *Eurotherm Conference No. 95: Computational Thermal Radiation in Participating Media IV*, Nancy, France, 2012.
- [16] A. Klar, J. Lang and M. Seaid, "Adaptive Solutions of SPn Approximations to Radiative Heat Transfer in Glass," *International Journal of Thermal Sciences*, vol. 44, pp. 1013-1023, 2005.
- [17] M. F. Modest, J. Cai, W. Ge and E. Lee, "Elliptic Formulation of the Simplified Spherical Harmonics Method in Radiative Heat Transfer," *International Journal of Heat and Mass Transfer*, vol. 76, pp. 459-466, 2014.
- [18] J. E. Morel, J. M. McGhee and E. W. Larsen, "A 3-D Time-Dependent Unstructured Tetrahedral-Mesh SPn Method," *Nuclear Science and Engineering*, vol. 123, pp. 319-327, 1996.
- [19] S. Pautz, B. Bohnhoff, C. Drumm and W. Fan, "Parallel discrete ordinates methods in the SCEPTRE project," in *International Conference on Mathematics, Computational Methods & Reactor Physics (M&C 2009)*, Saratoga Springs, NY, 2009.
- [20] H. C. Edwards, "Sierra framework for massively parallel adaptive multiphysics applications," in *Proceedings from the NECDC 2004*, Livermore, CA, 2004.
- [21] A. L. Crosbie and R. G. Schrenker, "Radiative transfer in a two-dimensional rectangular medium exposed to diffuse radiation," *Journal of Quantitative Spectroscopy and Radiative Transfer*, vol. 32, no. 4, pp. 339-372, 1984.
- [22] Z. Altac and M. Tekkalmaz, "Solution of the radiative integral transfer equations in rectangular participating and isotropically scattering inhomogeneous medium," *International Journal of Heat and Mass Transfer*, vol. 47, pp. 101-109, 2004.